

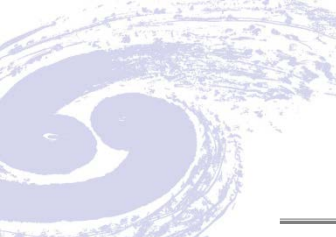
Amplitude Analysis of the Decays $\eta' \rightarrow \pi^+ \pi^- \pi^0$ and $\eta' \rightarrow \pi^0 \pi^0 \pi^0$

M. Ablikim,¹ M. N. Achasov,^{9,c} X. C. Ai,¹ O. Albayrak,⁵ M. Albrecht,⁴ D. J. Ambrose,⁴⁴ A. Amoroso,^{49a,49c} F. F. An,¹ Q. An,^{46,a} J. Z. Bai,¹ R. Baldini Ferroli,^{20a} Y. Ban,³¹ D. W. Bennett,¹⁹ J. V. Bennett,⁵ M. Bertani,^{20a} D. Bettoni,^{21a} J. M. Bian,⁴³ F. Bianchi,^{49a,49c} E. Boger,^{23,c} I. Boyko,²³ R. A. Briere,⁵ H. Cai,⁵¹ X. Cai,^{1,a} O. Cakir,^{40a} A. Calcaterra,^{20a}



Introduction

Based on a sample of 1.31×10^9 J/ψ events collected with the BESIII detector, an amplitude analysis of the isospin-violating decays $\eta' \rightarrow \pi^+ \pi^- \pi^0$ and $\eta' \rightarrow \pi^0 \pi^0 \pi^0$ is performed. A significant P -wave contribution from $\eta' \rightarrow \rho^\pm \pi^\mp$ is observed for the first time in $\eta' \rightarrow \pi^+ \pi^- \pi^0$. The branching fraction is determined to be $\mathcal{B}(\eta' \rightarrow \rho^\pm \pi^\mp) = (7.44 \pm 0.60 \pm 1.26 \pm 1.84) \times 10^{-4}$, where the first uncertainty is statistical, the second systematic, and the third model dependent. In addition to the nonresonant S -wave component, there is a significant σ meson component. The branching fractions of the combined S -wave components are determined to be $\mathcal{B}(\eta' \rightarrow \pi^+ \pi^- \pi^0)_S = (37.63 \pm 0.77 \pm 2.22 \pm 4.48) \times 10^{-4}$ and $\mathcal{B}(\eta' \rightarrow \pi^0 \pi^0 \pi^0) = (35.22 \pm 0.82 \pm 2.54) \times 10^{-4}$, respectively. The latter one is consistent with previous BESIII measurements.



$$J/\psi \rightarrow \gamma \eta' \quad \text{and} \quad \eta' \rightarrow \gamma \rho, \quad \rho \rightarrow \pi\pi/\gamma\pi\pi, \quad \pi^0 \rightarrow \gamma\gamma$$

For $J/\psi \rightarrow \gamma \eta'$ with $\eta' \rightarrow \pi^0 \pi^0 \pi^0$,

$$\eta' \rightarrow \pi^+ \pi^- \pi^0$$

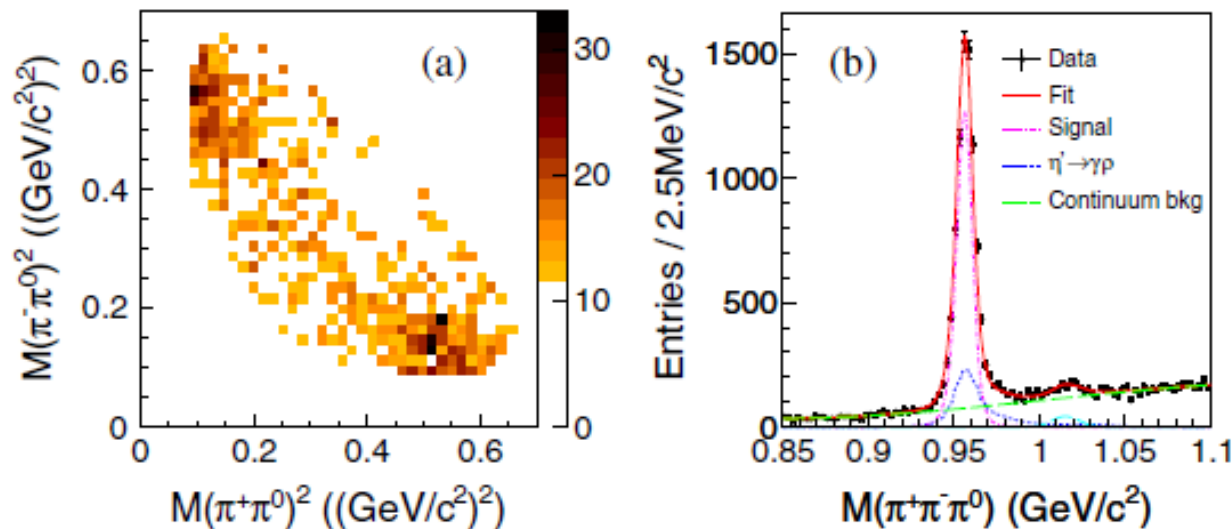


FIG. 1. (a) $\eta' \rightarrow \pi^+\pi^-\pi^0$ Dalitz plot for candidate events selected from data. (b) Invariant mass distribution of $\pi^+\pi^-\pi^0$ candidates without the η' mass constraint applied in the kinematic fit.

With the above requirements, a sample of 8267 events is selected, and the corresponding Dalitz plot is shown in Fig. 1(a), where two clusters of events corresponding to the decays of $\eta' \rightarrow \rho^\pm\pi^\mp$ are observed. The possible back-

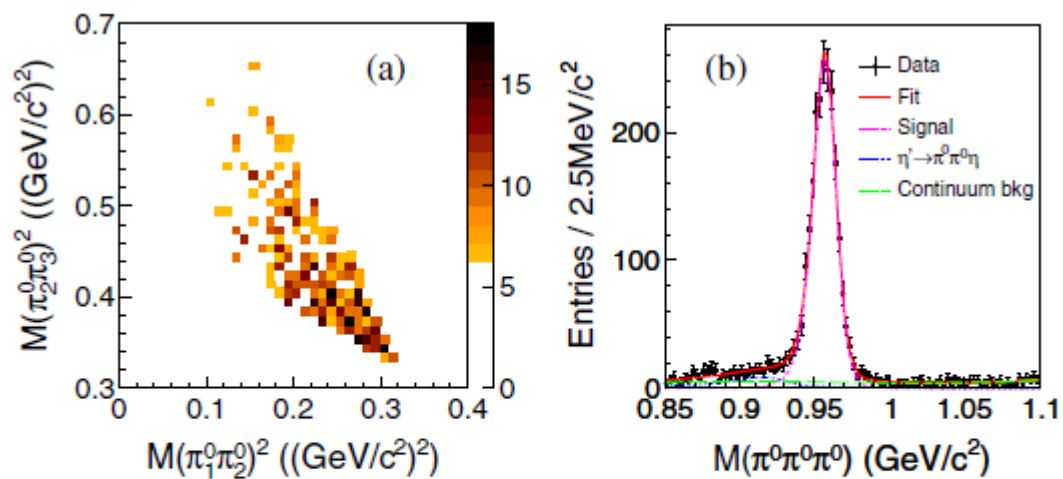
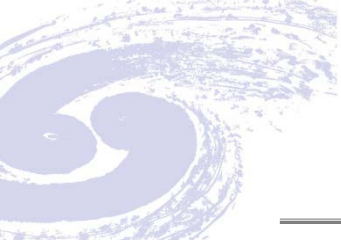
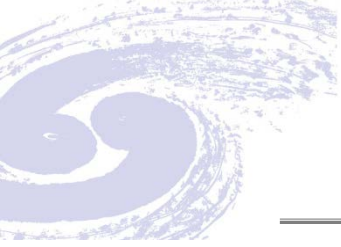


FIG. 2. (a) $\eta' \rightarrow \pi^0 \pi^0 \pi^0$ Dalitz plot for candidate events selected from data. (b) Invariant mass of $\pi^0 \pi^0 \pi^0$ candidates without the η' mass constraint applied in the kinematic fit.



A Dalitz plot analysis based on the formalism of the isobar model [23] is performed. The resonant $\pi\text{-}\pi S$ -wave ($L = 0$ for σ) and P -wave ($L = 1$ for ρ^\pm) amplitudes are described following the formalism from Ref. [24],

$$W(s) = \frac{1}{\cot\delta_L(s) - i}, \quad (1)$$

where

$$\begin{aligned} \cot\delta_0(s) &= \frac{\sqrt{s}}{2k} \frac{M_\pi^2}{s - M_\pi^2/2} \left(\frac{M_\pi}{\sqrt{s}} + B_0^S + B_1^S \omega_0(s) \right), \\ \cot\delta_1(s) &= \frac{\sqrt{s}}{2k^3} (M_\rho^2 - s) \left(\frac{2M_\pi^3}{M_\rho^2 \sqrt{s}} + B_0^P + B_1^P \omega_1(s) \right), \\ \omega_L(s) &= \frac{\sqrt{s} - \sqrt{s_L - s}}{\sqrt{s} + \sqrt{s_L - s}} - 1. \end{aligned}$$

Here s is the $\pi\pi$ invariant mass square, $k = \sqrt{s/4 - M_\pi^2}$, $\sqrt{s_0} = 2M_K$, the masses M_ρ , M_K , and M_π are fixed to the world average values [20], $\sqrt{s_1} = 1.05$ GeV is a constant, and B_0^S , B_1^S , B_0^P , and B_1^P are free parameters.

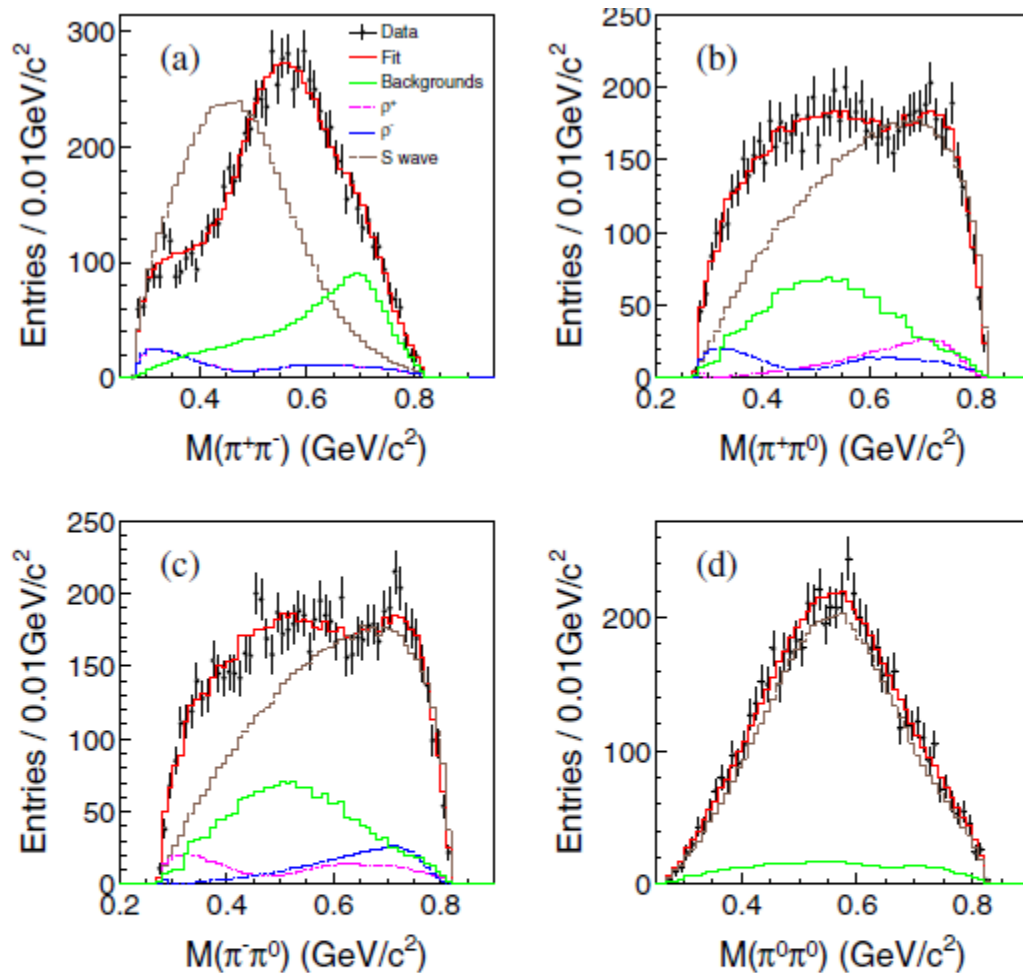
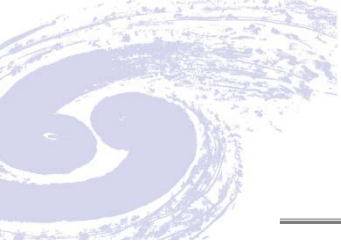


FIG. 3. Comparison of the invariant mass distributions of (a) $\pi^+\pi^-$, (b) $\pi^+\pi^0$, (c) $\pi^-\pi^0$, and (d) $\pi^0\pi^0$ between data (dots with error bars) and the fit result projections (solid histograms). The dotted, dashed, dash-dotted, and dash-dot-dotted histograms show the contributions from background, S wave, ρ^- , and ρ^+ , respectively.

TABLE I. Yields with statistical errors, detection efficiencies, and branching fractions for the studied η' decay modes, where the first errors are statistical, the second systematic, and the third model dependent.

Decay mode	Yield	ϵ (%)	\mathcal{B} (10^{-4})
$\pi^+\pi^-\pi^0$	6067 ± 91	25.3	$35.91 \pm 0.54 \pm 1.74$
$\pi^0\pi^0\pi^0$	2015 ± 47	8.8	$35.22 \pm 0.82 \pm 2.54$
$\rho^\pm\pi^\mp$	1231 ± 98	24.8	$7.44 \pm 0.60 \pm 1.26 \pm 1.84$
$(\pi^+\pi^-\pi^0)_S$	6580 ± 134	26.2	$37.63 \pm 0.77 \pm 2.22 \pm 4.48$

TABLE II. Summary of systematic uncertainties for the determination of branching fractions for each component.

Source	$\rho^\pm\pi^\mp$ (%)	$(\pi^+\pi^-\pi^0)_S$ (%)	$\pi^+\pi^-\pi^0$ (%)	$\pi^0\pi^0\pi^0$ (%)
Constraint	15.9	3.3
MDC tracking	2	2	2	...
Radiative photon	1	1	1	1
π^0 selection	2	2	2	6
Kinematic fit	1.7	1.7	1.7	1.6
Background	3.0	1.4	1.2	1.3
Number of J/ψ	0.8	0.8	0.8	0.8
$\mathcal{B}(J/\psi \rightarrow \gamma\eta')$	3.1	3.1	3.1	3.1
Total	16.9	5.9	4.9	7.2
Model	24.7	11.9



Summary

In summary, using a combined amplitude analysis of $\eta' \rightarrow \pi^+ \pi^- \pi^0$ and $\eta' \rightarrow \pi^0 \pi^0 \pi^0$ decays, the P -wave contribution from ρ^\pm is observed for the first time with high statistical significance. The pole position of ρ^\pm , $775.49(\text{fixed}) - i(68.5 \pm 0.2) \text{ MeV}$, is consistent with previous measurements, and the branching fraction $\mathcal{B}(\eta' \rightarrow \rho^\pm \pi^\mp)$ is determined to be $(7.44 \pm 0.60 \pm 1.26 \pm 1.84) \times 10^{-4}$.